

# Miniaturized Semi-Lumped UWB Bandpass Filter with Improved out-of-band performances

Darine Kaddour, Jean-Daniel Arnoult, and Philippe Ferrari

A miniaturized ultra wideband (UWB) bandpass filter with improved out-of band performances is presented in this paper. Based on the combination of low-pass and high-pass filters, the UWB filter is realized in a semi-lumped technology using microstrip transmission lines and surface mounted capacitors. In this paper, the filter design rules have been carried out. Furthermore, filters having a 3-dB fractional bandwidth of 142% centered at 0.77 GHz have been realized. Measurements in good agreement with simulations, show attractive properties of return loss ( $|S_{11}| < -18$  dB), insertion loss ( $< 0.3$  dB). Moreover, a technique adopting capacitively loaded stubs was used to extend the stopband till 8 times the center frequency.

## I. Introduction

Since the Federal Communications Commission (FCC)'s release of the frequency band from 3.1 to 10.6 GHz for commercial purposes [1], the UWB radio system has been receiving great attention from both academy and industry. As an essential component, UWB bandpass filters with good performances, compact size and easily-implemented structures are in high demand. So far, several prototypes of UWB filters have been reported.

In [2], a microstrip ring filter with the dual stopbands below 3.1 GHz and above 10.6 GHz was constructed to make up the most initial UWB filter. However, this filter in fact has many problematic issues, such as unexpected passbands below 3.1 GHz, narrow stopbands, large size and complex configuration.

Due to their geometric simplicity, parallel coupled microstrip lines were commonly used to design bandpass filters. Generally, this procedure is used for bandwidths less than about 20% [3]. To overcome this limitation, a three-coupled-line microstrip structure was proposed in [4] to design a bandpass filter with a fractional bandwidth of 50 %. However, the more the fractional bandwidth is required, the smaller the gap size is demanded to enhance the coupling. For UWB filter design, the necessary gap size is still too narrow to be fabricated. Furthermore, ground plane aperture compensation techniques were successfully used for significant increasing of coupling coefficient between parallel coupled lines leading thus to wider bandwidths [5-6].

Moreover, the stepped-impedance resonators (SIRs) demonstrated their advantageous efficiency for UWB bandpass filters. In [7], a UWB bandpass filter with five transmission poles is proposed using multiple-mode resonator (MMR). By properly allocating the first three resonance peaks quasi-equally within UWB band, a short-circuited coplanar waveguide (CPW) MMR bandpass filter is realized [8]. In [9], a two-stage UWB bandpass filter is presented. The capacitive-ended interdigital coupled-line topology is adopted to achieve improved out-of-band per-

formance. Note that the filters in [7] and [9] lack of design method and synthesis procedure. Later, modified stub-loaded multiple-mode resonator were proposed in [10-13] aiming to allocate the first resonant frequencies within 3.1-10.6 GHz band while suppressing spurious harmonics at the upper-stopband. In [14], quasi-Chebyshev bandpass filter with nine transmission poles is synthesized using three triple-mode SIRs two-layer broadside-coupled structure. Ground plane aperture techniques, increasing coupling between pairs MMR resonators, were also widely investigated to improve the out-band rejection in UWB filters [14-15].

Furthermore, stub bandpass filters with several configurations could be also used to meet UWB mask requirements [16-19]. In [16-17] connecting lines between short-circuited stubs were meandered in order to reduce the filter size. These UWB filters have sharp rejection, but their spurious response would degrade the out-of-band response and an increase in number of sections may lead to large insertion loss, as well as poor group delay. Besides, stepped impedance open stubs were implemented on this kind of structures to realize transmission zeros and get sharper attenuations [18-19].

In addition, tight coupling in a microstrip to CPW or slotline transition has also been investigated [20-24]. The use of microstrip-to-CPW transition has received great attention providing a wide bandpass operation with a good trade-off in terms of insertion loss and group delay flatness [20]. In [21], the UWB filter with a multiple-mode resonator was proposed using the microstrip-to-CPW transitions as inverter circuits. Composite transition lines exhibiting cross-coupling and slow-wave behavior were later proposed in [22], leading to more compact devices. Recently, back-to-back microstrip-slotline cross-junction transition is rearranged to make up a novel class of UWB bandpass filter with lenient tolerance in fabrication [23-24].

Basically, a wide bandwidth filter may be implemented by a direct cascade of the low- and high-pass filters. In [25], the wideband coplanar-waveguide (CPW) bandpass filters based on the cascade of CPW low- and high-pass periodic structures were constructed. To save the circuit area, a high-pass filter realized by shunt quarter-wave short-circuited stubs is embedded with a stepped-impedance low-pass filter [26]. As a result of the use of low degree high-pass filter, the filter lacked selectivity or sharpness at the lower frequency. Note that a suspended stripline technology combining low loss with reduced size was also used to fabricate this composite filter [27]. Analytical techniques to synthesize an isolated cascade of high- and low-pass sections based on an iterative algorithm for both Butterworth and Chebychev cases were also reported in [27]. In our previous work [kaddour, EUMA], several UWB filters were realized in a semi-lumped approach using both surface mounted (SMT) capacitors and microstrip transmission lines. Thanks to the slow-wave behavior introduced by capacitively loaded transmission lines, a high degree of miniaturization is demonstrated in [29].

In this paper, a technique of spurious suppression is studied. The paper is organized as follows. First, a design method is carried out and validated by simulations in section II. Then, several planar filters with 3-dB fractional bandwidth of 142 % centered at 0.77 are designed in section III. Measurement and simulation results are in very good agreement. The insertion loss is limited to less than 1 dB in the passband, and the maximum group delay variation is 1.6 ns. Furthermore, a spurious suppression technique using capacitively loaded stubs is introduced. Consequently, the first spurious frequency appears at more than eight times the center frequency when a 40-dB out-of-band attenuation is considered. Finally, twisted capacitively loaded stubs are used to minimize the circuit size (55%) providing a good agreement between measurements and simulations.

## II. Principle

### A) Configuration and synthesis technique

Figure 1 shows the equivalent electrical circuit of the semi-lumped proposed UWB bandpass filter. Following the same principle as in [26], a low-pass and a high-pass filters are combined. The high-pass filter is realized by shunt quarter-wave short-circuited stubs. The stepped impedance low-pass filter used in [26] is replaced in this work by a low-pass filter based on capacitively loaded transmission lines as published in [29]. Comparing with the distributed filter [26], a size reduction reaching 85% was demonstrated thanks to the use of the semi-lumped technology [Kaddour, EUMA]. In addition, two series capacitors are added at the near- and far- ends of the filter in order to give more sharp rejection around the lower stopband.

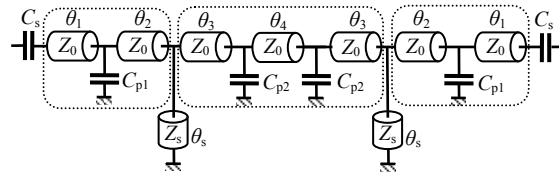


**Figure 1. Equivalent electrical circuit of the proposed semi-lumped UWB filter.**

In order to investigate the synthesis procedure, an UWB filter centered at 0.77 GHz with a 142% relative 3-dB bandwidth, is considered. In this paper, the center frequency  $f_c$  of the bandpass filter is given by:

$$f_c = \sqrt{f_L f_H} \quad (1)$$

where  $f_L$  and  $f_H$  are respectively the low and high 3-dB cut-off frequencies.

The proposed synthesis procedure concerns the establishment of a rough initial estimation of the filter's parameters, by setting both low and high cut-off frequencies. To simplify the study, an initial design with ideal transmission lines and capacitors is adopted. In addition, identical series transmission lines' electrical lengths are first considered, i.e.  $\theta = \theta_1 = \theta_2 = \theta_3 = \theta_4$ . The main advantage of this filter topology is the independent control of both low and high cut-off frequencies. The upper and lower cut-off frequencies are respectively controlled by the low-pass and high-pass sections.

The low-pass sections are realized by capacitively loaded transmission lines following the same principle of the low-pass filters published in [29]. In this previous work, the low-pass section has been studied and the design equations relating the characteristic impedance  $Z_0$ , the loading capacitance  $C_p$ , the transmission line electrical length  $\theta$  to the cut-off frequency  $f_H$  were derived. For a characteristic impedance equal to  $120 \Omega$  and assuming a 1.5 GHz high cut-off frequency, the equations established in [29] lead to  $C_p = 3.1 \text{ pF}$  and  $\theta = 29^\circ @ 1.5 \text{ GHz}$ .

While the high cut-off frequency  $f_H$  is adjusted by the low-pass section, the low cut-off frequency  $f_L$  is directly controlled by the short circuited stubs electrical length  $\theta_s$ . For thus, a simple tuning carried out with Agilent ADS [30] revealed that the electrical length  $\theta_s$  should be set to  $23^\circ @ 0.4 \text{ GHz}$ .

Currently, rough initial values for  $C_p$ ,  $\theta$  and  $\theta_s$  are available. The filter response simulated using the following parameters ( $C_p = 3.1 \text{ pF}$ ,  $\theta = 29^\circ @ 1.5 \text{ GHz}$ ,  $\theta_s = 23^\circ @ 0.4 \text{ GHz}$ ) is illustrated in Figure 2. As a result, the obtained cut-off frequencies are 0.4 GHz and 1.45 GHz, respectively. So the simple design method described above is sufficient for a rough estimation of the filter's parameters. Note that the simulated filter suffers also from a poor matching in the passband with a return loss reaching only 8 dB around 1.3 GHz. However, the return loss will be improved in the second step of the design when the filter will be optimized.

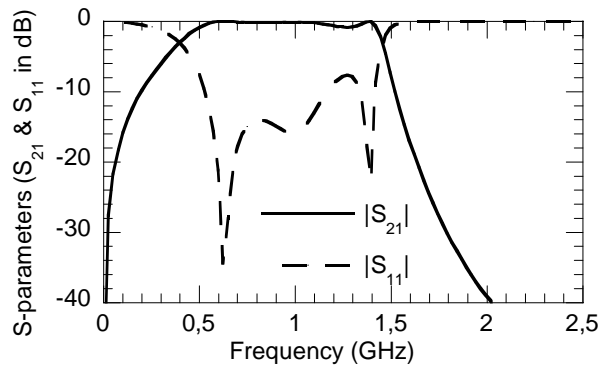


**Figure 2. Simulation response of the UWB bandpass filter with  $C_p = 3.1 \text{ pF}$ ,  $\theta_H = 29^\circ @ 1.5 \text{ GHz}$ , and  $\theta_s = 23^\circ @ 0.4 \text{ GHz}$ .**

For the second step consisting of a whole optimization of the complete filter, a microstrip technology is considered. A Rogers™ RO4003 substrate with relative permittivity  $\epsilon_r = 3.38$ , substrate thickness  $h = 813 \mu\text{m}$ , and dielec-

tric losses  $\tan\delta=0.0027$ , has been adopted. Also,  $T$  junctions, surface mounted capacitor's, soldering pads and via holes models are taken in account. Complete models taking into account the parasitic series elements with an inductance of 0.35 nH and a resistance of 0.25  $\Omega$  are considered to get more accurate simulation responses. In order to maximize freedom degrees and improve filter performances, the series transmission lines' electrical length and the capacitors' value are no more considered as equal.

The UWB filter is optimized using Agilent ADS [30]. The transmission lines characteristic impedance has been set to 120  $\Omega$ , leading to a strip width  $W_{hi}$  equal to 250  $\mu\text{m}$ . The value for the series capacitors added in the near- and far-end of the UWB bandpass filter to improve the low stop-band rejection is fixed to 6.8 pF, leading to a small impedance compared to 50  $\Omega$ , keeping unchanged the low cut-off frequency. Table 1 lists the electrical lengths and capacitor's values obtained after optimization for the UWB filter. Figure 3 gives the simulation results to 8 GHz. As illustrated, return loss is better than 20 dB in the whole passband, and insertion loss is limited to 0.2 dB at the center frequency. The shape factor, defined between -3 dB and -20 dB, equals 1.3:1. In the simulated response, spurious frequency occurs around 5 GHz, leading to an out-of-band rejection level of -40 dB to only 4.5 GHz, i.e. 4.5 times the center frequency. The study of the spurious origin is carried out in the next section where a simple original technique to reject these spurious frequencies is suggested.

**Table 1. Electrical lengths and capacitors' values of the proposed UWB semi-lumped bandpass filters.**

$\theta_1(^{\circ})$	$\theta_2(^{\circ})$	$\theta_3(^{\circ})$	$\theta_4(^{\circ})$	$\theta_5(^{\circ})$	$C_{p1}$ (pF)	$C_{p2}$ (pF)	$C_s$ (pF)
7	17	6	26	12	1.8	3.9	6.8

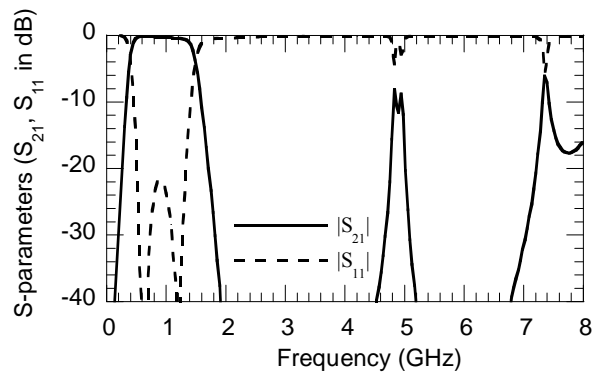


**Figure 3. Simulation response of the bandpass filters using parameters' values given in Table 1.**

### B) Spurious analysis and improvement

The basic principle of spurious suppression is based on the transmission zeros repartition in the frequency response. As illustrated in Figure 4, three transmission zeros are observed respectively at 2.2, 3.2, and 6 GHz. So a possible solution to reject the spurious frequencies and improve the rejection band width could be to move the

transmission zeros, either to push the 3.2 GHz transmission zero to higher frequencies, or to pull the 6 GHz transmission zero to lower frequencies. Therefore, the study of the origin of these transmission zeros has to be carried out first.

Transmission zeros located at 2.2 GHz and 3.2 GHz are due to the resonance of the LC shunt circuit formed by the SMT capacitor and the parasitic inductances. This parasitic inductance is the sum of the intrinsic SMT capacitor's, the soldering pads, and the via holes inductances. Considering the capacitor's model and the via hole's dimensions, its value  $L_s$  can be estimated to 1.3 nH. The transmission zero location is then easily calculated using the expression of the LC resonant frequency:

$$f_r = \frac{1}{2\pi\sqrt{L_s C_{pi}}} \quad (2)$$

Indeed, the 2.2-GHz transmission zero is introduced by the resonant circuit formed by the 3.9-pF capacitor and the series parasitic inductance  $L_s=1.3$  nH, while the 3.2-GHz transmission zero is related to 1.8-pF capacitor. As the high cut-off frequency is controlled by the LC circuit, the lower transmission zeros could not be moved. A modification of these transmissions zeros will affect the passband response of the UWB filter.

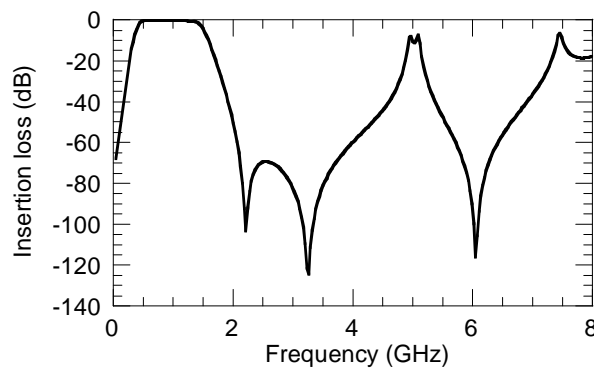


**Figure 4. Transmission zeros of the UWB bandpass filter till 8 GHz.**

The transmission zero appearing at 6 GHz is due to the short-circuited stub resonance that presents a  $180^\circ$  electrical length near to 6 GHz. A solution for spurious suppression would be to pull this transmission zero to lower frequencies. This could be easily achieved by increasing the stub electrical length. However, as the low cut-off frequency is fixed by the stub's length, the low frequency electrical length should not be modified. Thus, capacitively loaded stubs could be successfully used for spurious suppression, leading to the whole UWB bandpass filter equivalent electrical circuit given in Figure 5. A capacitively loaded stub will behave as an unloaded stub at low frequency because the capacitor's susceptance is high, so that the stub's behavior remains unchanged. When the frequency will increase, the loading capacitor becomes significant compared to the stub's transmission line

distributed capacitor, and the wave velocity in the loaded stub will decrease, leading to a lower resonant frequency for the stub.

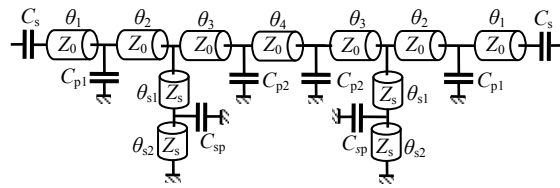


**Figure 5. UWB filter equivalent electrical circuit with capacitively loaded stubs.**

Using Agilent ADS [30], the UWB filter with capacitively loaded stubs has been optimized. The electrical lengths ( $\theta_{s1}$  &  $\theta_{s2}$ ) and the stub's loading capacitor  $C_{sp}$  optimized values have been and set respectively to  $5^\circ$  and  $11^\circ$  and  $0.4$  pF. The equivalent electrical length of both loaded ( $\theta'_s$ ) and unloaded ( $\theta_s$ ) stubs are plotted in Figure 6. While the unloaded stub electrical length increases proportionally versus frequency, the loaded stub electrical length increases quickly with frequency, leading a lower resonant frequency of  $4.2$  GHz. Thus the transmission zero will be shifted to lower frequencies. In the lower band, the electrical length for both loaded and unloaded stubs are quite similar. So the filter passband remains quite unchanged with the capacitively loaded stubs configuration.

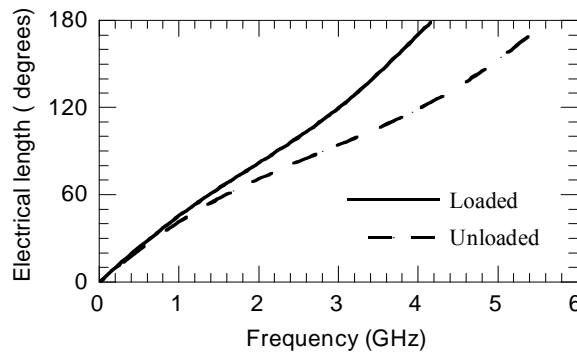


**Figure 6. Comparison of the electrical length of the capacitively loaded stub ( $C_{sp}=0.4$  pF) and the unloaded stub.**

Figure 7 compares the UWB filter insertion loss with both loaded and unloaded stubs. Whereas the filter response remains unchanged in the passband, the loading capacitor effect appears for higher frequencies. When the capacitively loaded stubs are used, the third transmission zero which was located at  $6$  GHz occurs now at  $3.8$  GHz, while the first two transmission zeros due to LC resonance remain fixed. Consequently, the high frequency rejection band, defined below an attenuation of  $-40$  dB, is enlarged to about  $6.5$  GHz, i.e. more than eight times the filter's center frequency of  $0.77$  GHz.

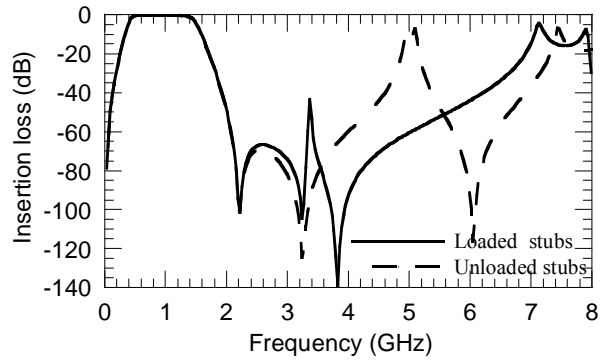


Figure 7. Simulated insertion loss for the UWB filter with loaded- and unloaded stubs.

### III. UWB filters realization & measurements

In this section, several UWB filters with 3-dB bandwidth of 142 % centered at 0.77 GHz are realized and measured. The photograph of the realized filters is given in Figure 8. Filters with loaded and unloaded stubs have been fabricated. For filters with loaded stubs, SMT (Figure 8.b) and patch (Figure 8.c) capacitors are considered. SMT capacitors with a 0402 case (0.5 mm by 1 mm) have been used. All the realized filters are 3.7 cm- length.

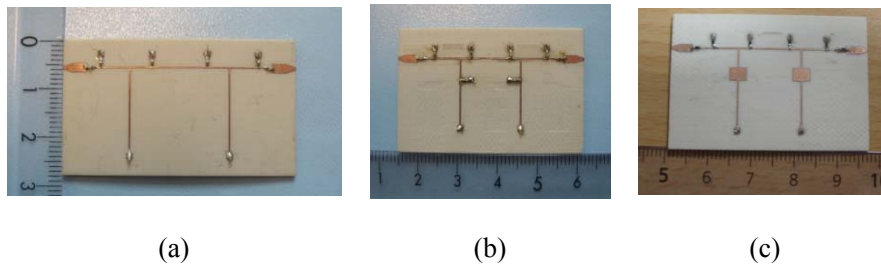
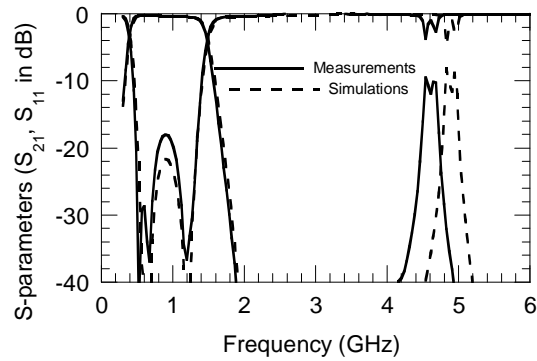


Figure 8. Photograph of the realized filters. a) Unloaded stubs. b) stubs loaded by SMT capacitors. c) stubs loaded by patch capacitors.

First, measurement and simulation results of the UWB filter with unloaded stubs are given in Figure 9. Comparison between the simulation and measurement results of the UWB filter with unloaded stubs. A good agreement is observed in the filter passband. A wideband of 1.1 GHz is achieved leading to the expected bandwidth of 142%. The measured return and insertion loss are found to be higher than 18 dB and lower than 0.3 dB over the passband, respectively. The first spurious response appears around 4.5 GHz. A slight shift of about 400 MHz is observed between simulations and measurements. This shift is probably due to the capacitor's model that is not sufficiently accurate at high frequencies. The measured rejection band, if a minimum 40-dB attenuation is considered, extends to about 4.2 GHz, i.e. 5.4 times the center frequency.



**Figure 9. Comparison between the simulation and measurement results of the UWB filter with unloaded stubs.**

Measurements of both filters with unloaded and loaded with SMT capacitors stubs are compared in Figure 10. While the bandwidth is quite the same for the two topologies, return loss is improved to 20 dB with the capacitively loaded stubs. With the introduction of SMT capacitors, the first spurious peak is shifted from about 4.5 GHz to 6.7 GHz. The measured rejection band (a minimum 40-dB attenuation is still considered) extends to about 6 GHz when capacitively stubs are used, i.e. more than eight times the center frequency, showing a significant improvement.

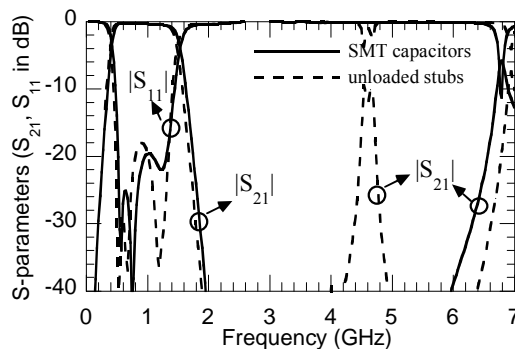


**Figure 10. Comparison between measured frequency responses, for both UWB filters with unloaded and loaded by SMT capacitors stubs.**

Next, Figure 11 gives the comparison between the measurement results to 8 GHz, for both filters with stubs loaded by SMT and patch capacitors. With patch capacitors, the return loss is better than 18 dB in the passband and the rejection band is slightly enlarged from 6 to 6.6 GHz. So it can be concluded that capacitively loaded stubs can be successfully used for spurious suppression.

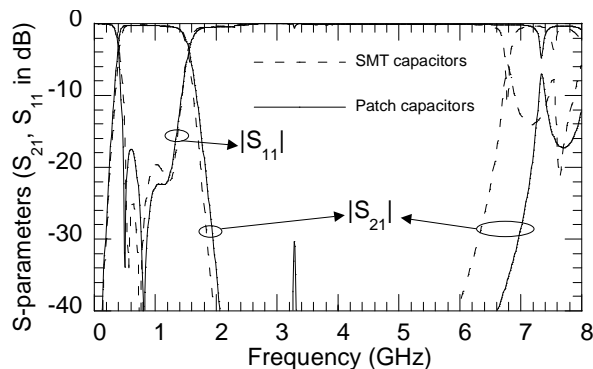


**Figure 11. Comparison between measured frequency responses, for both UWB filters with capacitively loaded stubs.**

For miniaturization purposes, bended stubs could be used. This technique could not be easily achieved with stubs loaded by patch capacitors. So, a filter with bended stubs loaded by SMT capacitors was fabricated. Figure 12 gives the photograph of the miniaturized filter. The miniaturization improvement with bended stubs reaches 55% (in term of surface) compared to the filter with straight stubs. A good agreement between measurement and simulation results is observed in Figure 12. Return loss is better than 22 dB and the rejection band extends to about 6 GHz.

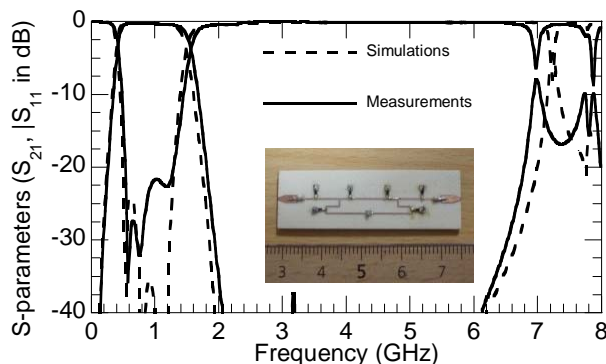


**Figure 12. Simulations and measurements response for the UWB filter with bended capacitively loaded stubs.**

## V. Conclusion

In this paper, a new topology of semi-lumped UWB bandpass filter has been proposed. It is based on the combination of a low-pass and a high-pass filters. The synthesis method of the bandpass filter has been developed and validated by simulations. Filters centered at 0.77 GHz with a relative bandwidth of 142% have been designed and fabricated. Simulated and measured results have shown a good agreement in terms of return loss (better than 18 dB) and insertion loss, (lower than 0.3 dB). A spurious suppression technique, using capacitively loaded stubs, has been carried out and has demonstrated its efficiency to eliminate spurious responses until more than eight times the center frequency. A miniaturization better than 55% has also been achieved by a simple stub bending.

## References

1. FCC, "Revision of Part 15 of the commission's Rules regarding Ultra-Wide-Band Transmission System," *Technical Report ET-Docket 98-153*, 14 February 2002.
2. H. Ishika and K. Araki, "A design of tunable UWB filters," *International Workshop Ultra Wideband Systems*, Kyoto, 18-21 May 2004, pp. 424-428.
3. K.-S. Chin, L.-Y. Lin, and J.-T. Kuo, "New formulas for synthesizing microstrip bandpass filters with relatively wide bandwidths," *IEEE Microwave Wireless Components Letters*, Vol. 14, No. 5, May 2004, pp. 231-233.
4. J.-T. Kuo, and E. Shih, "Wideband bandpass filter design with three-line microstrip structures," *2001 IEEE MTT-S International Microwave Symposium Digest*, Phoenix, AR/USA, pp. 1593-1593.
5. Y.A. Kolmakov, and I.B. Vendik, "Compact ultra- wideband bandpass filter with defected ground plane," *35th European Microwave Conference*, October 2005, Paris, France.
6. M.-K. Mandal, and S. Sayal, "Compact wideband bandpass filter," *IEEE Microwave Wireless Components Letters*, Vol. 16, No. 1, January 2006, pp. 46-48.
7. L. Zhu, S. Sun, and W. Menzel, "Ultra-wideband (UWB) bandpass filters using multiple-mode resonator," *IEEE Microwave Wireless Components Letters*, Vol. 16, No. 11, November. 2005, pp. 796-799.
8. J. Gao, L. Zhu, W. Menzel, and F. Bögelsack, "Short-circuited CPW multiple-mode resonator for ultra-wideband (UWB) bandpass filter," *IEEE Microwave Wireless Components Letters*, Vol. 16, No. 3, March 2006, pp. 104-107.
9. S. Sun and L. Zhu, "Capacitive-ended interdigital coupled lines for UWB bandpass filters with improved out-of-band performances," *IEEE Microwave Wireless Components Letters*, Vol. 16, No. 8, August 2006, pp. 440-443.
10. S.-T. Li, and Q.-X. Chu, "A compact UWB bandpass filter with improved upper-stopband performance," *International Conference on Microwave and Millimeter Wave Technology*, April 2008, pp. 363 - 365.
11. S. W. Wong, and L.Zhu, "Ultra-wideband (UWB) microstrip bandpass filters with improved upper-stopband and miniaturized size," *Asia-Pacific Microwave Conference*, December 2007.
12. S. W. Wong, and L.Zhu, "EBG-embedded multiple-mode resonator for UWB bandpass filter with improved upper-stopband performance," *IEEE Microwave Wireless Components Letters*, Vol. 17, No. 6, June. 2007, pp. 421-424.
13. R. Li, and L. Zhu, "Compact UWB bandpass filter using stub-loaded multiple-mode resonator," *IEEE Microwave Wireless Components Letters*, Vol. 17, No. 1, January 2007, pp. 40-43.
14. J.-T. Kuo, Y.-C. Chiou and E. Cheng, "High selectivity ultra-wideband (UWB) multimode stepped-impedance resonators (SIRs) bandpass filter with two-layer broadside-coupled structure," *Asia-Pacific Microwave Conference*, December 2007.
15. H. Wang and L. Zhu, "Aperture-backed microstrip line multiple-mode resonator for design of a novel UWB bandpass filter," *Asia-Pacific Microwave Conference*, December 2005.
16. W.-T. Wong, Y.-S. Lin, C.-H. Wang, and C.H. Chen, "Highly selective microstrip bandpass filters for ultra-wideband (UWB) applications," *Asia-Pacific Microwave Conference*, December 2005.
17. H. Shamman, and J-S. Hong, "A novel ultra-wideband (UWB) bandpass filter (BPF) with pairs of transmission zeroes," *Microwave Wireless Components Letters*, Vol. 17, No. 2, February 2007, pp. 121-123.
18. P. Cai, Z. MA, X. Guan, X. Yang, Y. Kobayashi, T. Anada, and G. Hagiwara, "A compact UWB bandpass filter using two-section open-circuited stubs to realize transmission zeros," *Asia-Pacific Microwave Conference*, December 2005.
19. X. Gong, J. Wang, and W. Wang, "An improved design method for UWB filter using two-section open-circuited stubs," *International Conference on Microwave and Millimeter Wave Technology*, April 2007.
20. K. Li, D. Kurita, and T. Matsui, "An ultra-wideband bandpass filter using broadside-coupled microstrip-coplanar waveguide structure," *2005 IEEE MTT-S International Microwave Symposium Digest*, pp. 675-678.
21. H. Wang, L. Zhu, and W. Menzel, "Ultra-wideband bandpass filters with hybrid microstrip/CPW structure," *IEEE Microwave Wireless Component Letters*, Vol. 15, No. 12, December 2005, pp. 844-846.
22. T.-N. Kuo, S.-C. Lin and C.H. Chen, "Compact ultra-wideband filters using composite microstrip-coplanar-waveguide structure," *IEEE Transactions on Microwave Theory and Techniques*, Vol. 54, No. 10, October 2006, pp. 3772-3778.
23. R. Li, and L. Zhu, "Ultra-wideband (UWB) bandpass filters with hybrid microstrip/slotline structures," *IEEE Microwave Wireless Component Letters*, Vol. 17, No. 11, November 2007, pp. 778-781.
24. R. Li, and L. Zhu, "Compact UWB bandpass filter on hybrid microstrip/slotline structure with improved out-of-band performances," *International Conference on Microwave and Millimeter Wave Technology*, April 2008.
25. Y. S. Lin, W. C. Ku, C. H. Wang, and C. H. Chen, "Wideband coplanar-waveguide bandpass filters with good stopband rejection," *IEEE Microwave Wireless Component Letters*, Vol. 14, No. 9, September 2004, pp. 422-424.
26. C. L. Hsu, F. C. Hsu, and J. T. Kuo, "Microstrip bandpass filter for ultra-wideband (UWB) wireless communications," *2005 IEEE MTT-S International Microwave Symposium Digest*, pp. 679-682.
27. W. Menzel, M. Tito, and L. Zhu, "Low-loss ultra-wideband (UWB) filters using suspended stripline," *Asia-Pacific Microwave Conference*, December 2005.
28. R. Gomez-Garcia, and J.I. Alonso, "Systematic method for the exact synthesis of ultra-wideband filtering responses using high-pass and low-pass sections," *IEEE Transactions on Microwave Theory and Techniques*, Vol. 54, October 2006, pp. 3751-3764.

29. D. Kaddour, E. Pistono, J.-M. Duchamp, J.-D. Arnould, H. Eusebe, P. Ferrari, and R.-G. Harrison, "A compact and selective low-pass filter with reduced spurious responses, based on CPW tapered periodic structures," *IEEE Transactions on Microwave Theory and Techniques*, Vol. 54, June 2006, pp. 2367-2375.
30. ADS. Agilent Technologies. Inc. Headquarters, 395 Page Mill Rd. Palo Alto, CA 94306, USA.
31. LPFK Laser & Electronics AG, Osteriede 7, D-30827 Garbsen, Germany, [lpfk@lpfk.de](mailto:lpfk@lpfk.de).